JOURNAL OF PROPULSION AND POWER
Vol. 17, No. 6, November–December 2001

Strutjet Engine Performance

Bryan T. Campbell,* Adam Siebenhaar,† and Thong Nguyen‡
Aerojet, Sacramento, California 95813-6000

To increase the technology readiness level of hypersonic scramjet technology, an innovative strut-based dual-mode ramjet engine design capable of powering a hypersonic vehicle at speeds from Mach 4 to 8 is investigated. Two versions of the engine are under development: a dual-mode (ramjet/scramjet) engine for missile applications and a rocket-based combined cycle engine for space access. This paper will discuss the features of the dual-mode engine design and how they contribute to overall engine performance. Engine component performance was evaluated using a combination of analysis and component testing. Inlet performance data (mass capture, pressure recovery, and inlet/isolator pressure ratio) were obtained from wind-tunnel testing and correlated with model and full-scale computational fluid dynamics (CFD) analyses. Combustor performance data (combustion efficiency, fuel-injection performance, and pressure distributions) were obtained from full-scale direct-connect combustor testing. Nozzle losses and efficiency were obtained from CFD analysis. Performance parameters derived from these component tests and analyses were fed into a standard hypersonic engine cycle code to predict flight engine performance. The demonstrated component performance values were extrapolated to determine predicted component performance at the end of engine development, which were used to compute the vision flight engine performance.

Nomenclature

Fn/Wa = specific thrust, thrust/airflow rate, lb_f-s/lb_m
I_{sp} = specific impulse, thrust/fuel flow rate, lb_f-s/lb_m

Introduction

THE dual-mode strutjet engine program is concentrated on development, integration, and demonstration of the technologies necessary to establish the technology base for liquid hydrocarbon fueled scramjet propulsion systems capable of powering hypersonic vehicles at speeds from Mach 4 to 8. This engine is designed to operate using both subsonic (ramjet mode) and supersonic (scramjet mode) combustion of hydrocarbon fuel with air in a single flowpath. The features of this engine result in high performance with built-in margin. During the course of the engine development reported here, this performance was demonstrated through component testing and computational fluid dynamics (CFD) analysis. A vehicle concept utilizing the dual-mode strutjet engine is pictured in Fig. 1. The features of the engine, which enable high performance, are shown in Fig. 2. The main features are the streamwise struts in the flowpath, which enhance performance in several ways. The three-dimensional compression effect of the struts decreases forebody turning requirements to achieve a given amount of compression, reducing inlet losses. In the combustor the struts provide a smaller flowpath for each fuel injector to feed (i.e., a smaller mixing gap), thereby improving fuel distribution and mixing. The increased surface area of the inlet increases friction losses; however, a net benefit is provided because there is an increase in the static pressure of the airstream entering the combustor. A higher combustion pressure improves combustion efficiency for a given combustor length yielding higher thrust.

An additional performance improvement is attained from the cascade injectors, which are supersonic injection nozzles with a low-drag-shaped exit. These injectors are designed to provide high penetration along with good fuel atomization and distribution. The injectors are distributed throughout the flowpath in order to allow tailoring of fuel delivery for different operating conditions. Coupled with the decreased mixing gap caused by the struts, fuel/air mixing is greatly enhanced compared to standard injectors. This allows the use of a shorter, lighter combustor to obtain a given amount of thrust. Additional description of the cascade injectors is presented in the combustor section.

Cooling of the engine is required to maintain structural integrity. This is accomplished through a combination of radiation and regenerative cooling.[1] Hot gases in the combustor heat the composite engine shell (C/SiC), which radiates to a cold plate (see Fig. 2) and cooling fins inside the hollow struts. The hydrocarbon fuel (n-decane) is circulated through the cold plate and cooling fins to remove the heat. In addition, the fuel is endothermic[1]; hence, when it is heated it goes through a chemical reaction which absorbs heat, increasing the cooling capability of the system. Tests showed minimal coke formation in the small channels of the platelet cold plate.[1]

The modular nature of the strutjet brought about by the struts facilitates engine scaling. The engine can be easily scaled by adding more flowpaths without requiring fueling redistribution because each flowpath is identical. Additionally, scaling in this manner does not change the boundary-layer characteristics relative to the flowpath geometry. These two factors simplify the scaling procedure for use on alternate vehicles.

Flowpath Details and Component Testing

A schematical side view of the strutjet flowpath is shown in Fig. 3. The struts provide additional compression, allowing self-start at ramjet takeover (Mach 3.8) at a higher contraction ratio than possible with a two-dimensional inlet. Although the extra surface area of the struts in the isolator section does produce friction losses, these losses also increase the flow static pressure. High static pressure in the combustor is beneficial and necessary for combustion. Because the static pressure rises more quickly than in a two-dimensional inlet, the isolator section can be made shorter, resulting in a lighter engine. The combustor combines high-performing cascade injectors, a recessed flameholding cavity, and a decreased mixing gap provided by the struts. A high-efficiency nozzle expands the flow to produce thrust. The major components of the strutjet engine are discussed next.

Inlet/Isolator

The role of the inlet is to capture air and prepare it for combustion. The isolator is a section of flowpath that separates the inlet and the

Revision received 26 November 2000; accepted for publication 29 December 2000.

*Senior Engineer, Liquid Propulsion Products, P.O. Box 13222; bryan.campbell@aerojet.com. Member AIAA.

†Team Leader, Propulsion and Armaments, P.O. Box 13222; adam.siebenhaar@aerojet.com. Member AIAA.

‡Technical Principal, Propulsion and Armaments, P.O. Box 13222; thong.nguyen@aerojet.com. Member AIAA.

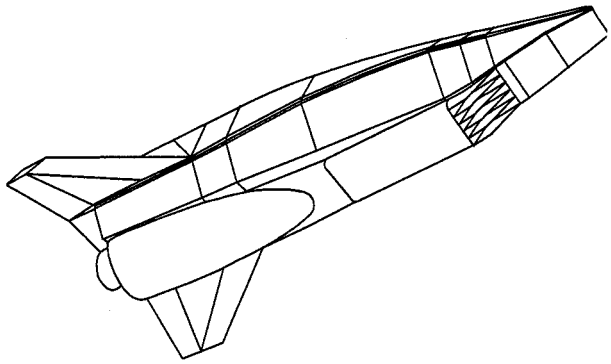

Fig. 1 Strutjet missile vehicle concept.

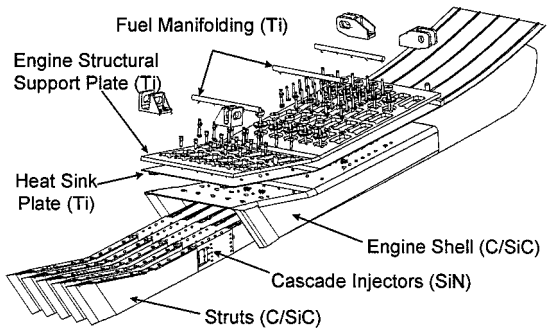

Fig. 2 Exploded view of strutjet engine.

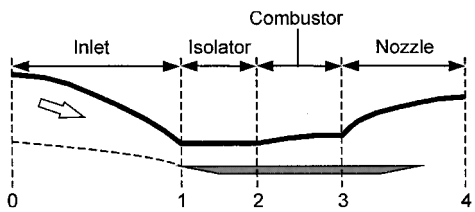

Fig. 3 Strutjet flowpath schematic.

combustor. The isolator acts as a diffuser, which decelerates and raises the pressure of the flow through a series of oblique shocks (the "shock train").[2] The shock train is formed as the pressure in the combustor is raised from the inlet stream value. This high pressure feeds upstream in the subsonic boundary-layer flow in the isolator, eventually causing separation of the wall boundary layer caused by the adverse pressure gradient. This separated flow, in turn, produces a shock wave that reflects down the flowpath. This shock system causes total pressure losses with an accompanying increase in static pressure. As the combustion pressure is raised, the shock system can move upstream until it reaches the inlet plane, causing a drastic loss in air capture (inlet "unstart"). Friction and heat loss also contribute to the static pressure change through the duct. For supersonic flow friction causes an increase in static pressure (Fanno flow), whereas heat loss produces a decrease in static pressure (Rayleigh flow).[3] Hence, the function of the inlet/isolator combination is to capture air and raise its static pressure to the level needed by the combustor.

The presence of struts in the flowpath raises the friction losses per unit length. Friction creates two results: Drag and static pressure increase (supersonic Fanno flow). Drag is of course a penalty because it decreases the net thrust of the engine. However, the friction-induced increase in static pressure is beneficial to the engine and aids the inlet/isolator in performing its function. Hence, not as much shock-related pressure rise is required, decreasing the length of the shock train and associated isolator length. This results in a shorter engine with lower weight. The magnitudes of these changes are sensitive to the particulars of each design. However, with a proper design, the inlet/isolator section can be shorter than a no-strut design for the same combustion pressure, resulting in a lighter engine.

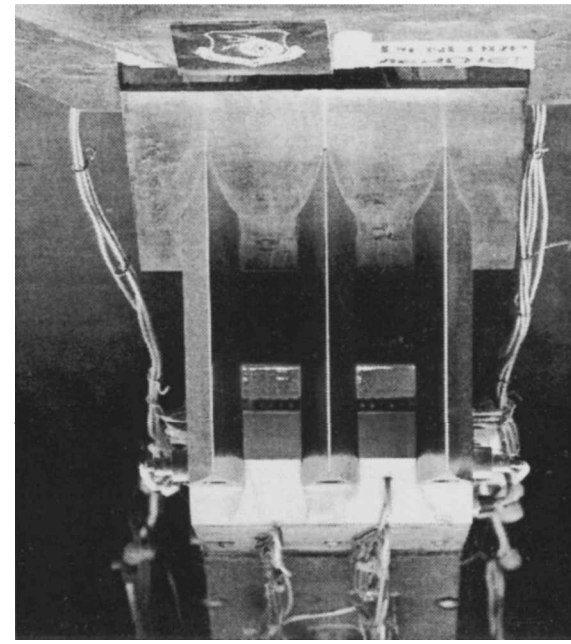

Fig. 4 60% scale strutjet inlet test model.

During the course of the dual-mode engine development, experimental and computational investigations of the strutjet inlet performance were performed. Experiments on a 60% scale strutjet inlet (shown in Fig. 4) were conducted in a 1×1 ft (0.305×0.305 m) supersonic wind tunnel. This continuous-flow facility can test models at Mach numbers from 1.3 to 6. Interchangeable two-dimensional nozzles are used to vary the facility Mach number. Because of facility constraints on test model size, inlet tests were performed without the vehicle forebody. Hence, the facility Mach number was adjusted to match the approach conditions of the inlet (i.e., after the forebody). Testing of the strutjet inlet was done at facility Mach numbers of 3.5, 4, 5, 5.5, and 6, which simulated flight Mach numbers from 4 to 8. High combustion pressures are simulated using a flow plug to raise the pressure at the flowpath exit (i.e., inlet backpressure). A small amount of forebody bleed (about 1% of mass flow) is utilized on the strutjet inlet design to improve performance by stabilizing the forebody boundary layer. This feature was incorporated in the wind-tunnel model using a small vertical step with an axial gap vented to a low-pressure region. Several experimental techniques (duct pressure maps, pitot rake, boundary-layer pitot probe, cowl spillage cone probe, video Schlieren, and oil-flow visualization) were used to characterize the performance of the inlet. The tests demonstrated consistent self-start at the Mach 4 condition with a fixed geometry. High mass capture and pressure ratio were also demonstrated at this critical Mach number (ramjet takeover). In addition, there was a gradual drop in mass capture as the inlet started to spill at the maximum backpressure ("soft" unstart), which led to minimal hysteresis for inlet restart. A "soft" unstart characteristic is beneficial for a flight system because it provides warning of impending inlet unstart and allows flight avionics to make appropriate adjustments to prevent loss of thrust. Mass capture exceeding initial goals was demonstrated at all Mach numbers tested, benefiting low-Mach-number thrust production. Good backpressure capability was demonstrated and several geometry modifications (e.g., bleed slot, cowl angle) were investigated for potential performance improvement. Testing at Mach 6 was complicated by facility interactions, which prevented achievement of maximum performance. Because of schedule constraints and the desire to complete the more important Mach 8 testing (i.e., cruise condition), no attempts were made to correct the facility problems and completion of Mach 6 testing was postponed. Pitot rake surveys showed consistent exit mass-flow distributions across the test Mach-number range, indicating that vertical changes in fuel

injection location as a function of flight conditions may not be necessary. In all, nearly 1000 readings of inlet instrumentation were taken.

Full Navier–Stokes CFD simulations of both flight and subscale strutjet inlets were performed at freestream Mach numbers of 4, 6, and 8. Subscale computations without the forebody were anchored to the test results to validate CFD codes. Simulations at both the wind-tunnel and flight conditions were performed with several geometry options and backpressure levels. The objectives were to determine capture efficiency, inlet pressure recovery (kinetic energy efficiency), combustor entrance static pressure (pressure ratio), and spill drag. Additionally, a validated computational methodology is crucial to inlet design optimization. Good agreement was seen at Mach 4 and 6 for both capture and backpressure ratio (there was no test at Mach 8). Mass capture agreed within about 3%, and Mach 4 pressure ratio agreed within 4%. Pressure ratio results at Mach 6 showed better performance with the CFD model than in the experiment (about 20% higher). This is consistent with the problems just mentioned, which were encountered during Mach 6 testing. Axial pressure distributions also matched well between CFD and test, and the cone probe inlet spillage measurements agreed with the CFD computed spillage.

Combustor

Several features of the strutjet combustor contribute to high performance. The struts provide ideal sites for fuel injectors and decrease the individual flowpath size. This results in a smaller mixing gap as shown in Fig. 5. The strutjet combustor injects fuel into the gaps between the struts, while a classical two-dimensional engine injects fuel from the top and bottom of the flowpath. Because the strut gap is typically smaller than the flowpath height, the mixing gap is reduced. Hence each injector has a smaller portion of the flowpath cross section to fuel, and fuel distribution can be optimized as opposed to fuel penetration. Use of strut-mounted fuel injectors also simplifies fuel line routing because no fuel injectors are used on the cowl side of the flowpath. A schematic of the combustor strut is shown in Fig. 6. A forward cavity contains several liquid injectors that provide a pilot for the downstream injectors. The recessed cavity causes much less drag than an exposed piloting technique. Two sets of gas injectors and a set of liquid injectors are used with the fuel being routed to different injectors depending on flight conditions. Gas injectors are utilized at higher Mach numbers when the fuel

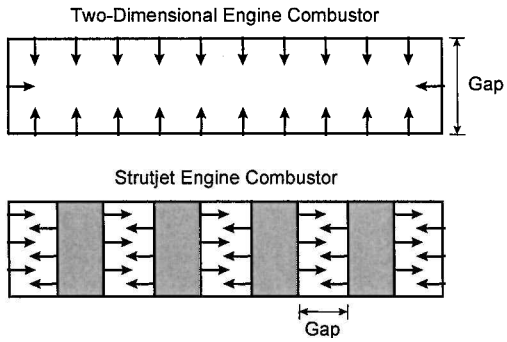

Fig. 5 Struts provide smaller mixing gap.

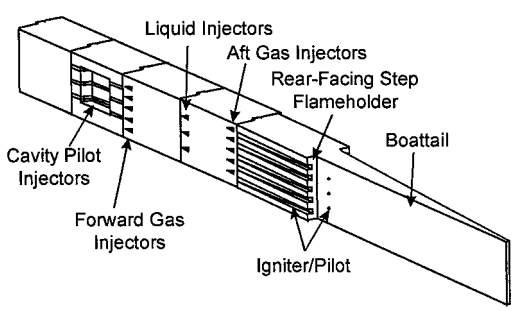

Fig. 6 Strut schematic.

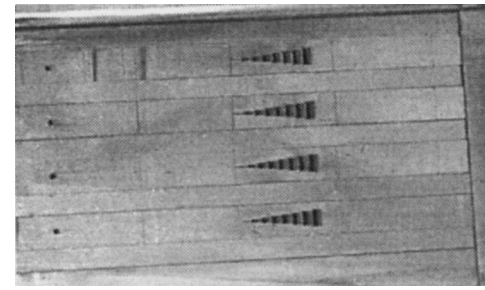

Fig. 7 Cascade injector.

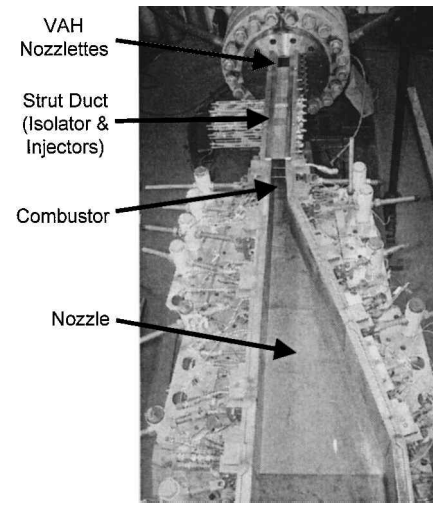

Fig. 8 Direct-connect combustor test rig.

becomes vaporized in the regenerative cooling system. The rear of the strut has a boat tail, a rearward facing step, and several mixing notches. Injectors in the region of the rearward facing step provide fuel for flameholding in the separated region downstream of the step. The boat tail provides a gradual area change in flow area that supports combustion. Distribution of the injectors both axially and vertically in the combustor allows for tailoring of fueling depending on flight conditions (i.e., during vehicle acceleration). Also note that injectors can be concentrated to account for a bias in the mass-flow distribution (i.e., flow distortion). The injectors utilized in the strutjet engine are high-performance cascade injectors,[4] shown in Fig. 7. The cascade injector provides better penetration and mixing than a conventional injector and reduces concentrated wall heat flux upstream of the injection site because the separated region upstream of the injector is smaller than that of a conventional injector. Elimination of these hot spots in turn reduces the complexity of the cooling system.

Sixty hot-fire tests of a full-scale dual-mode strutjet combustor were done in a direct-connect combustor test rig (see Fig. 8) at simulated flight conditions for Mach 4, 6, and 8. A vitiated air heater heated the supply air to the proper enthalpy to simulate high-Mach-number, high-altitude flight. The vitiated air passed through a converging-diverging nozzle to achieve the proper Mach number at the inlet of the strut duct.

Modular test hardware allowed variation of many fueling parameters. The injector blocks and cavity block shown in Fig. 6 were tested in various axial locations to determine the optimum fueling configuration and optimum combustor performance for each Mach-number regime. Each injector block was composed of injector wafers and spacers; therefore, the fuel injectors could be sited in nearly any desired location and configuration. The injector wafers were fabricated using the platelet process,[5] whereby thin metal sheets are etched and bonded together, forming complex internal manifolding. Combustor flight hardware would be manufactured using the same process, allowing for fuel routing inside the struts to accommodate

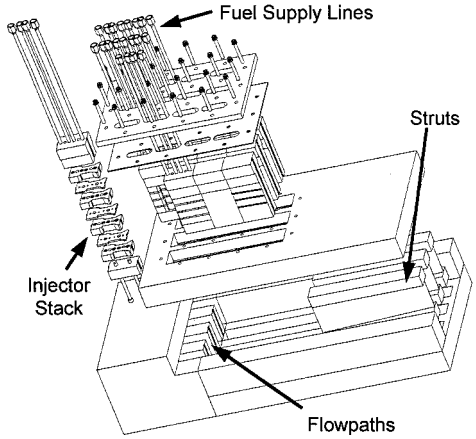

Fig. 9 Reconfigureable combustor test hardware.

shifts in fueling distribution during vehicle acceleration. Figure 9 is an exploded view of the strut assembly showing the injector stacks and fuel lines. Fueling flow rates and sequence were also varied to determine the optimum fueling scheme. The combustor/nozzle section of the test hardware was varied to adjust the area change of the flowpath. Flowpath area progression is a sensitive parameter for any scramjet engine, and the adjustable combustor/nozzle walls allowed investigations of the engine performance changes with area progression.

The direct-connect test program focused on Mach 4 and 8 testing. Mach 4 is critical as it is the ramjet takeover condition, while Mach 8 is the cruise condition. Extensive testing at Mach 6 was postponed as a result of scheduling issues. Testing at Mach 4 flight conditions achieved sustained engine operation with heated (~300°F) liquid decane fuel ($C_{10}H_{22}$) and a small amount of hydrogen flameholding in the boat-tail region. High combustion efficiency was demonstrated at an equivalence ratio of 0.75. This met the initial combustion efficiency goal for Mach 4 and was somewhat short of the 0.8 equivalence ratio goal. Mach 8 testing accomplished sustained combustion with simulated cracked decane (about 65% $C_{10}H_{22}$ and 35% C_2H_4) and required no additional fuels as combustion aids. The cavity pilot required only cold liquid decane fuel. Again, high combustion efficiency was demonstrated at an equivalence ratio of 0.78. This performance exceeded the initial combustion efficiency goal for Mach 8 while falling short of the 1.0 equivalence ratio goal. This engine performance was realized within a combustor length of 60 in., the goal for initial development. With some flowpath modifications guided by test results, further improvements in equivalence ratio should be realized. More details of the dual-mode combustor test program can be found in Ref. 6.

Nozzle

The nozzle contour was designed using the computer code RAO.[7] The required inputs are the nozzle entrance (i.e., combustor exit) height, nozzle exit height, nozzle length, and entrance flow conditions. The entrance flow conditions—Mach number, specific heat ratio, total temperature, and total pressure—are assumed to be uniform and were obtained from previous ramjet cycle code results for Mach 6 flight conditions. Nozzle optimization at Mach 6 was chosen as a trade between low-Mach-number performance at ramjet takeover and the Mach 8 cruise condition.

Nozzle performance was calculated using the commercial CFD code RAMPANT. The computed nozzle performance losses are given in Table 1. This calculation shows that the nozzle divergence loss is very small, approximately 0.05%, and that a majority of the performance loss is attributed to wall friction (2.65%). Thus, a small reduction in nozzle length will likely result in better overall nozzle performance. Figure 10 shows, in addition to nozzle length, other design parameters and features, which can be varied to optimize nozzle performance. Nozzle length is a trade between divergence loss and friction loss while nozzle-exit area is a trade between over/underexpansion losses at low and high speed. Figure 11 shows relative specific impulse I_{sp} vs flight Mach number for different nozzle area ratios. Increasing nozzle-exit area increases I_{sp} at higher speed, but decreases I_{sp} at lower speeds. Nozzle-exit geometry should be adjusted to optimize mission I_{sp}. Because the nozzle design was determined to have the lowest risk, no nozzle test program was planned for the initial development phase of the dual-mode engine.

Table 1 Nozzle loss breakdown

Loss mechanism	Value, %
Divergence	0.05
Upper and lower wall friction	1.41
Side wall friction	1.24
Total loss	2.7

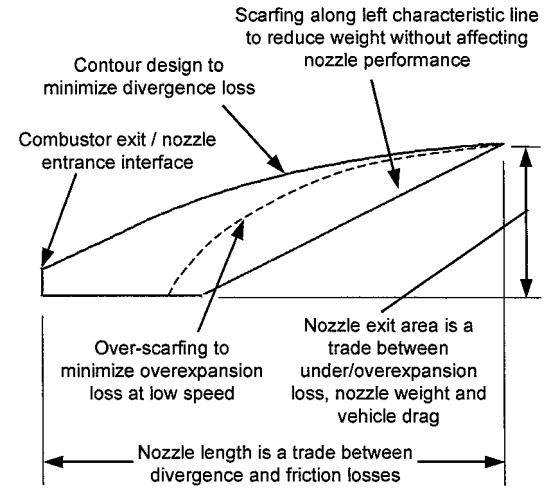

Fig. 10 Factors affecting nozzle performance.

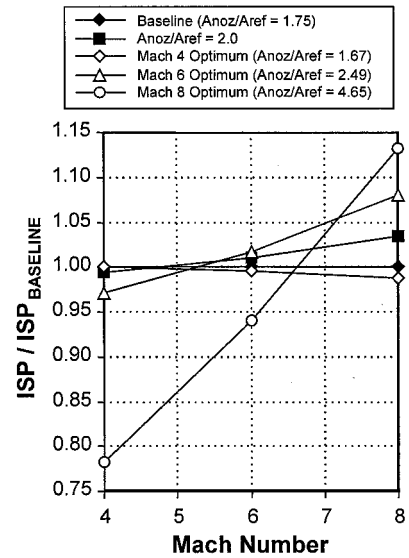

Fig. 11 Nozzle performance trade.

Performance Methodology

A methodology flowchart used in the engine performance assessment is given in Fig. 12. Overall engine performance was calculated using the Ramjet Performance Analysis computer code (RJPA), an industry-standard cycle-based code for predicting ramjet and scramjet performance.[8] This code requires input of component performance parameters such as inlet capture area (related to capture efficiency), inlet kinetic energy efficiency or total pressure recovery (i.e., total pressure loss in the inlet/isolator), combustion efficiency,

Table 2 Input parameters for baseline engine performance (phase I)

Parameter	Source	Values used in phase I performance assessment M = 4	M = 6	M = 8	Units
Dynamic pressure	Flight M and altitude	2000	2000	1000	lb_f/ft^2
Inlet capture efficiency	CFD + phase-I inlet tests	61.2	80.2	95.1	%
Inlet kinetic energy efficiency	CFD + phase-I inlet tests	95.0	94.3	97.5	%
Combustor wetted area	Engine geometry	1771	1771	1771	in^2
Combustion efficiency	Phase-I D.C. test data	NR[a]	NR[a]	NR[a]	%
Combustor friction coefficient	Phase-I D.C. test data	0.0017	0.0020[b]	0.0030	——
Equivalence ratio	Phase-I D.C. test data	0.75	0.8	0.78	——
Precombustion pressure ratio	Phase-I D.C. test data	2.25	4.04	3.63	——
Combustor heat loss	Analysis	154.8	198.2	192.8	Btu/s
Nozzle efficiency	CFD/W.L. direction	97	97	97	%
Nozzle kinetic efficiency (frozen-to-equilibrium)	W.L. direction	2:1	2:1	2:1	——

[a]NR indicates not released to the public. [b]Indicates values estimated as a result of insufficient test data at Mach 6 conditions. W.L. = Wright Laboratory. D.C. = Direct Connect.

Table 3 Phase I performance (%) achieved vs goals (100%)

Parameter	M = 4 Achieved	M = 4 Goal	M = 6 Achieved	M = 6 Goal	M = 8 Achieved	M = 8 Goal
I_{sp}, %	99.5	100.0	98.9	100.0	88.6	100.0
Fn/Wa, %	93.3	100.0	97.8	100.0	68.4	100.0
Equivalence ratio, %	92.5	100.0	100.0	100.0	78.0	100.0

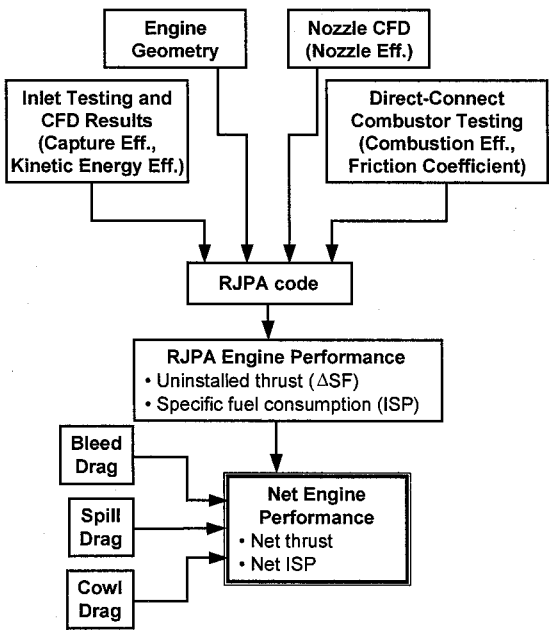

Fig. 12 Performance methodology flowchart.

combustor skin-friction coefficient, and nozzle efficiency. Component performance parameters were obtained from the testing (inlet and direct-connect combustor tests) and/or CFD analysis just discussed. The component performance parameters are functions of flight conditions (Mach number, dynamic pressure, angle of attack). The engine geometry and component performance parameters were input to RJPA, which predicted engine performance (thrust and I_{sp}) for different flight conditions. The sources for the major input parameters for engine performance computation are given in the flowchart (Fig. 12). Inlet capture area and kinetic energy efficiency were obtained from inlet tests as well as CFD computations. Combustion efficiency and combustor friction coefficient were obtained from the direct-connect testing, and combustor wall area is set by geometry. CFD analysis of the strutjet nozzle yielded an efficiency of 97%, and a 2:1 frozen-to-equilibrium chemistry ratio for the nozzle flow was assumed for the cycle performance calculations.

The engine thrust computed by RJPA is the difference between the stream thrusts evaluated at the nozzle exit and inlet capture plane (at the tip of the forebody). However, RJPA does not account for spillage, cowl, and bleed drags. These drag forces, which are functions of flight Mach number, flight dynamic pressure, and angle of attack, are calculated separately and subtracted from the RJPA-produced thrust to arrive at net values for engine thrust, I_{sp}, and thrust coefficient. Only form drag is included in the cowl drag calculation because all external friction drag is accounted for in vehicle drag. These sources of drag are subtracted from the thrust computed by RJPA to produce a net thrust and I_{sp}. These values were tabulated as functions of flight Mach number, flight dynamic pressure, angle of attack, and throttle setting to compute flight trajectories to meet the required mission profile.

Engine Performance

The dual-mode engine development program consists of three phases. Performance goals are approached in an incremental fashion such that component and system design improvements between each phase result in increased overall engine performance. The phase 1 engine is termed the baseline engine, phase 2 represents an intermediate step with increased performance, and the phase 3 engine is the vision flight engine. Performance of the baseline engine is computed using the methodology just outlined with the component performance values determined through testing and analysis. Extrapolation of baseline component performance to future designs was based on prior experience and allowed predictions of vision flight engine performance.

Baseline Engine Performance (Phase I)

Table 2 shows the values of the major input parameters used for calculation of phase I engine performance. A majority of these inputs were derived from test results. Capture efficiency and kinetic energy efficiency were computed by CFD analysis and were validated by inlet test results. Combustion efficiency, combustor friction coefficient, equivalence ratio, and precombustion pressure ratio were measured in the direct-connect combustor tests. Subscale inlet test results were confirmed for the flight vehicle using a CFD code that was anchored to test results. Preliminary nozzle performance was verified with CFD. Only a few direct-connect tests were devoted to Mach 6; therefore, the values for friction coefficient and combustion efficiency used in the performance analysis were estimated.

Table 3 gives the achieved phase I engine performance (computed using RJPA and the component performance values given in Table 2) along with the goals set for phase I performance. The

Table 4 Phase III I_{sp} and *Fn/Wa* projections expressed in percent improvements over end of phase I results

Parameter	Nozzle area ratio	M = 4	M = 6	M = 8
I_{sp}	1.75	18.8	25.1	39.3
Fn/Wa	1.75	57.9	56.8	80.8
I_{sp}	2.00	18.1	26.4	44.1
Fn/Wa	2.00	57.0	58.4	86.9

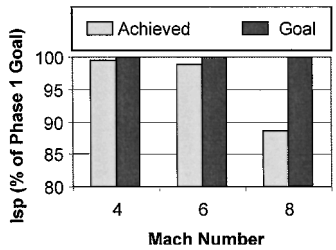

Fig. 13 Phase I specific impulses (%) vs Mach number.

phase I achieved I_{sp} values are plotted in Fig. 13 along with the goals. Overall, the phase I dual-mode strutjet engine performance computed with RJPA using component performance values evaluated with test data and CFD results compares favorably with the goals set for the initial phase of engine development.

Vision Flight Engine Performance (Phase III)

The component performance values determined by phase I testing were extrapolated to estimate component performance at the end of the dual-mode engine development (phase III) to estimate the performance of the final product, the vision flight engine. This extrapolation was based on previous experience of incremental performance gains attained through component and system design improvements and represented realistic estimations of future improvements in the performance of the individual engine components.

The goals for the vision flight engine component performance parameters are shown in Table 4. These goals represent realistic gains in component performance from the demonstrated phase I values that can be achieved in an incremental fashion by modifying component and system designs. The engine performance values presented in Table 4 are for two different nozzle area ratios (A_{exit}/A_{ref}) at cruise, 1.75 and 2.00. An area ratio of 1.75 was baselined; however, better cruise performance at Mach 8 can be achieved by raising the nozzle area ratio to 2.0 with less than 1% loss in performance at ramjet takeover (Mach 4) and a 1% gain in performance during acceleration at Mach 6.

Conclusion

The dual-mode strutjet engine has high performance and built-in margin and is easily scaled by adding additional flowpaths. Streamwise struts in the flowpath enhance overall performance by reducing inlet losses for a given amount of compression (i.e., less forebody turning required) and improving fuel distribution and mixing. Cascade injectors in the combustor provide low drag and high penetration for improved fuel atomization and mixing. Platelet fabrication processes enable complex fuel manifolding and routing inside struts, easily accommodating fueling and any required changes in fuel distribution during vehicle acceleration.

Component testing and CFD analysis were used to establish component performance parameters for the inlet/isolator, combustor, and nozzle. Overall flight engine performance was obtained from computations using the industry-standard ramjet/scramjet cycle performance analysis code and the component performance parameters derived from testing and analysis. The baseline dual-mode strutjet engine has good performance, nearly meeting most of the aggressive phase 1 goals. Beyond the baseline engine, there is a path for improving engine performance to meet the overall goals through modest component performance improvements, with no requirements for major technology breakthroughs in any areas. Thus, incremental component performance improvements will allow the engine to meet the performance goals.

Acknowledgments

The authors would like to thank the Air Force Research Laboratory HyTech Program Office for funding the development of the dual-mode strutjet engine through the Storable Fuel Scramjet Flowpath Concepts Program. Experiments on a 60% scale inlet were conducted in the 1 × 1 ft supersonic wind tunnel at the NASA John H. Glenn Research Center. Full-scale direct-connect combustor testing was performed by GASL Inc. Full Navier–Stokes CFD simulations of both flight and subscale inlets were performed by Boeing and Lockheed-Martin in support of this program.

References

[1]Chen, F. F., Tam, W. F., Shimp, N. R., and Norris, R. B., "An Innovative Thermal Management System for a Mach 4 to Mach 8 Hypersonic Scramjet Engine," AIAA Paper 98-3734, July 1998.

[2]Heiser, W. H., and Pratt, D. T., "Isolator-Combustor Interaction in a Dual-Mode Scramjet Engine," AIAA Paper 93-0358, Jan. 1993.

[3]Zucrow, M. J., and Hoffman, J. D., Gas Dynamics, Vol. 1, Wiley, New York, 1976, pp. 263, 315.

[4]Bulman, M., and Siebenhaar, A., "The Strutjet Engine: Exploding the Myths Surrounding High Speed Airbreathing Propulsion," AIAA Paper 95-2475, July 1995.

[5]Mueggenburg, H. H., Hidahl, J. W., Kessler, E. L., and Rousar, D. C., "Platelet Actively Cooled Thermal Management Devices," AIAA Paper 92-3127, July 1992.

[6]Siebenhaar, A., Bulman, M., Norris, R., and Thompson, M., "Development and Testing of the Aerojet Strutjet Combustor," AIAA Paper 99-4868, Nov. 1999.

[7]Nickerson, G. R., Dang, A. L., and Dunn, S. S., "The RAO Method Optimum Nozzle Contour Program," Software and Engineering Associates, Inc., Contract NAS8-36863, Carson City, NV, Feb. 1988.

[8]Pandolfini, P. P., Billig, F. S., Corpening, G. P., Corda, S., and Friedman, M. A., "Analyzing Hypersonic Engines Using the Ramjet Performance Analysis Code," APL Technical Review, Vol. 2, No. 1, 1990, pp. 68–78.